

## Supplementary

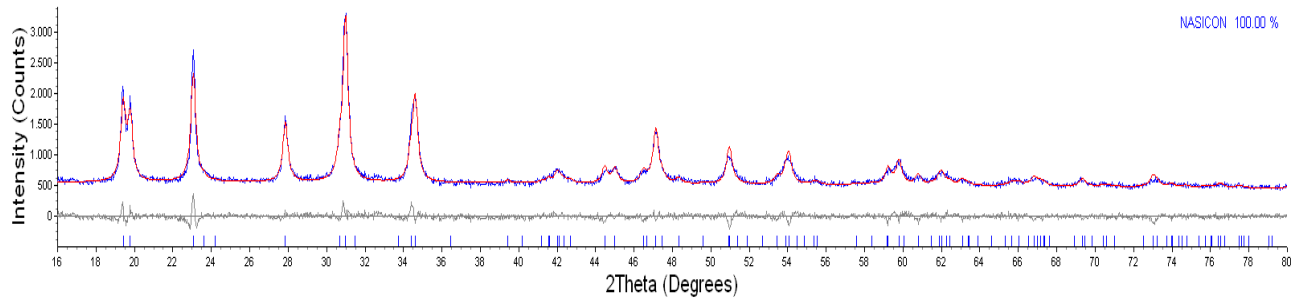


Figure S1. Rietveld refinement of the X-ray diffraction data of the p-MnZr sample. Experimental pattern (blue line), calculated pattern (red line), difference curve (grey line). Peaks position of the  $\text{Na}_3\text{MnTi}(\text{PO}_4)_3$  phase (blue bars on the bottom).

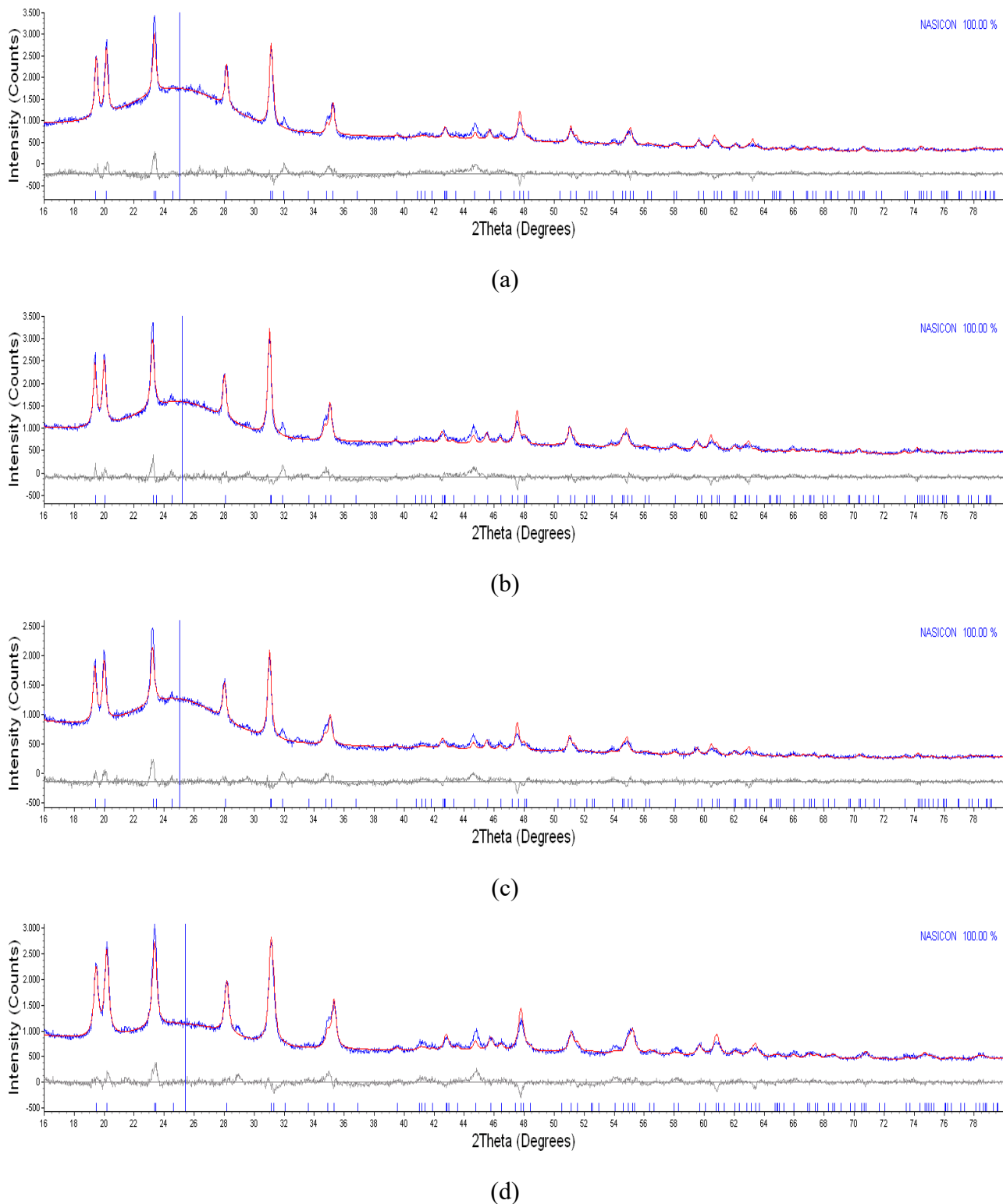


Figure S2. Rietveld refinement of the X-ray diffraction data of the a) h-10%MnZr/CNF, b) h-30%MnZr/CNF c) v-30%MnZr/CNF and d) dd-MnZr/CNF samples. Experimental pattern (blue line), calculated pattern (red line), difference curve (grey line). Peaks position of the  $\text{Na}_3\text{MnTi}(\text{PO}_4)_3$  phase (blue bars on the bottom). The refined position of the broad peak of the amorphous CNF phase is indicated by the blue vertical line.

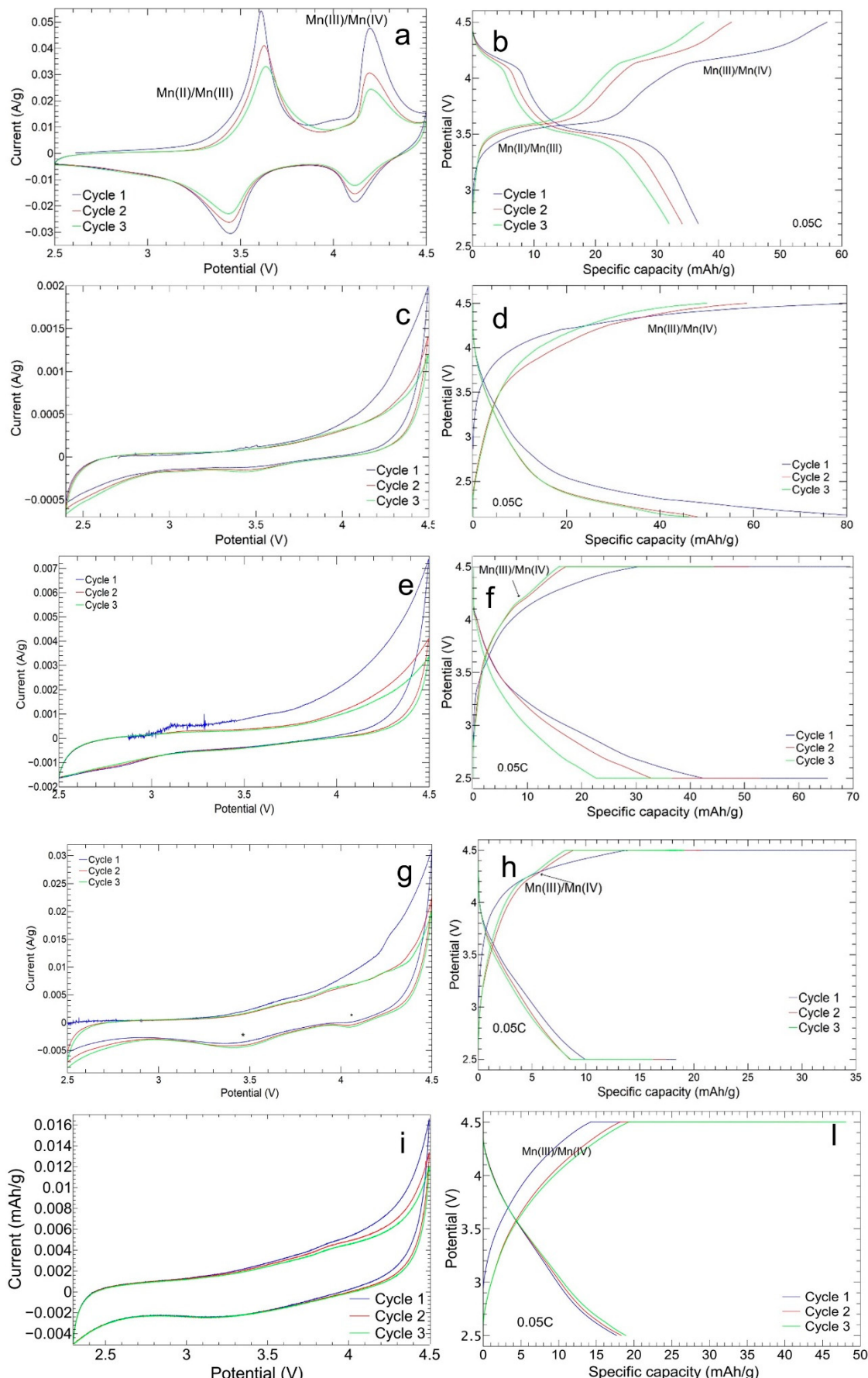


Figure S3. CV and charge/discharge curves of slurry p-MnZr (a,b), h-10%MnZr/CNF (c,d), h-30%MnZr/CNF (e,f), v-30%MnZr/CNF (g,h), and dd-MnZr/CNF (i,l) cathodes.

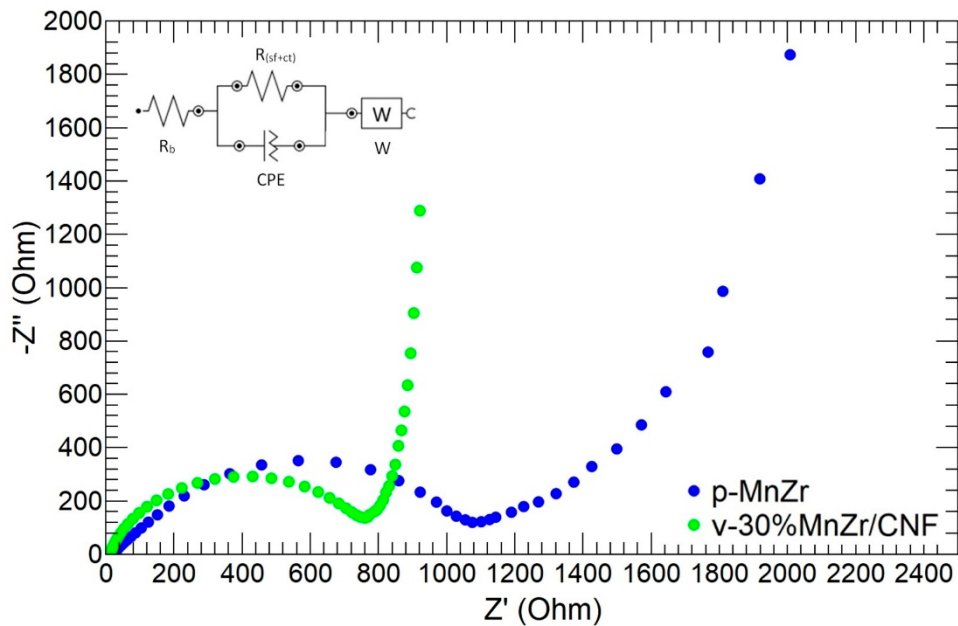


Figure S4. Nyquist plot of the v-30%MnZr/CNF and p-MnZr cathodes. The equivalent circuit is shown in the inset.  $R_b$ : electrolyte resistance;  $R_{(sf+ct)}$ : surface and charge transfer resistance;  $W$ : Warburg impedance.

Table S1. Refined lattice parameters, cell volume, crystallite size, weighted-pattern discrepancy factor and Goodness of Fit of the NASICON-structured  $\text{Na}_3\text{MnZr}(\text{PO}_4)_3$  phase obtained by Rietveld refinement of MnTi and MnTi/CNF samples.

SAMPLE	p-MnZr	dd-MnZr/CNF	h-10%MnZr/CNF	h-30%MnZr/CNF	v-30%MnZr/CNF
$a$ (Å)	8.970(1)	8.794(1)	8.818(1)	8.844(1)	8.840(1)
$c$ (Å)	22.585 (5)	22.742(4)	22.740(4)	22.705(4)	22.709(4)
$V$ (Å <sup>3</sup> )	175.45	173.20	173.66	173.90	173.85
$c/a$	2.518	2.586	2.578	2.567	2.569
Crystallite size (nm)	30(1)	28(1)	40(1)	37(1)	36(1)
<hr/>					
$R_{wp}$	5.51	6.26	6.67	6.13	6.79
S	1.41	1.75	1.83	1.76	1.62